Oxidation of Metals, Vol. 32, Nos. 5/6, 1989

Oxidation Kinetics of Chromium and Morphological Phenomena

E. A. Polman,* T. Fransen,*† and P. J. Gellings*

Received February 22, 1989; revised June 12, 1989

The oxidation kinetics of chromium at 900°C are independent of the oxygen partial pressure. Although this observation gives evidence for a defect mechanism where chromium interstitials account for the chromium transport in the oxide scale, the experimental phenomena do not support one single model. The occurrence of oxide whiskers and oxide ridges are explained by the energy of activation for the breakup of the oxidant molecule. Large oxide pegs are formed at metal multiple-grain junctions after scale breakdown.

KEY WORDS: chromium; oxidation; scale failure; scale morphology.

INTRODUCTION

The oxidation of chromium has been the object of many research programs because of the protective properties of chromia-forming steels. Kofstad and Lillerud[1,2] performed several experiments on the oxidation kinetics of chromium. The observed oxidation kinetics and the densification of chromia scales in vacuum were explained by a defect mechanism in which chromium interstitials determine the growth process. This model was supported by Hindham and Whittle[3] who found the oxidation kinetics of chromium at 1000°C in CO/CO_2 mixtures with by $2\times10^{-14} < P_{O_2} < 8\times10^{-9}$ bar to be independent of P_{O_2}.

*Department of Chemical Technology, University of Twente, P.O. Box 217, Enschede, The Netherlands.
†To whom all correspondence should be addressed.

0030-770X/89/1200-0433$06.00/0

This defect model seems in contrast with the Seebeck measurements of Young *et al.*[4] on sintered chromia. Young *et al.* doubt whether local equilibrium at the metal/oxide interface will be obtained, and assumed that chromium vacancies dominate the oxidation process. In this paper the results of oxidation experiments on chromium at 900°C over a wide range of oxygen partial pressures are reported and related to the several defect mechanisms proposed in the literature. Also, the morphology of the scales and phenomena, such as scale cracking, whisker formation, and selective grain-boundary oxidation, are discussed.

EXPERIMENTAL DETAILS

Chromium was received as lumps (Merck) and had a purity of 99.9%. The material was cut to rectangular samples ($\sim 20 \times 10 \times 2\ mm^3$). The samples were ground with emery paper (4000 grit), followed by a polishing treatment with Al_2O_3 (0.05 μm). Finally, they were ultrasonically cleaned in ethanol.

Oxidation tests were carried out in a Setaram thermobalance at 900°C in three different atmospheres: pure oxygen at 1 bar, a mixture of 1% CO in CO_2 with a calculated oxygen partial pressure of 1.0×10^{-2} bar, and a mixture of 1.5% H_2O in H_2 having an oxygen partial pressure of 9.8×10^{-21} bar. The H_2/H_2O mixture was prepared by saturating a hydrogen stream with water at 15°C.

Stripping of the oxide layers was performed in a solution of 10% Br_2 in methanol. The scanning electron microscopy (SEM) observations were carried out with a JEOL M35 CF instrument.

RESULTS

Oxidation Experiments

The results of the oxidation tests are presented in Fig. 1. The oxidation kinetics obey Wagner's parabolic rate law. The k_p values for O_2, 1% CO/CO_2, and 1% H_2O/H_2 are $(1.1 \pm 0.1) \times 10^{-11}$, $(2.1 \pm 0.7) \times 10^{-11}$, and $(1.5 \pm 0.1) \times 10^{-11}\ g^2\ cm^{-4}\ s^{-1}$ at 900°C, respectively. Although these values show some difference, they are all of the same order of magnitude.

Scale breakdown was not observed during the measurements, which were carried out at a constant temperature. Some measurements in oxygen were continued up to 50 hr, and no accelerated oxidation behavior, indicative of scale breakdown, was observed. Upon cooling, cracking may occur. Severe blistering of the scale after cooling at a rate of 30°C/hr was observed for scales formed in CO/CO_2.

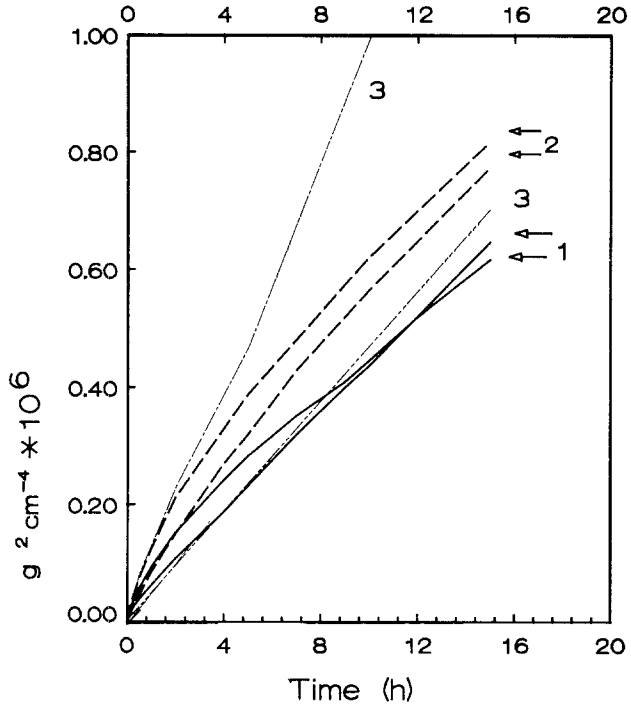

Fig. 1. The oxidation of chromium at 900°C; 1 = O_2, 2 = 1.5% H_2O/H_2, 3 = 1% CO/CO_2.

SEM Observations

The oxide formed after oxidation in pure oxygen, consists of very fine oriented grains. Figure 2 shows the surface of the oxide formed at 900°C after oxidation in pure oxygen for 15 hr. The grains may differ in size as can be seen in this figure. It is also obvious from Fig. 3 that the larger grains are built up of smaller grains by shared crystal faces. Because of this, it is impossible to determine the preferred crystallographic orientations of the chromia crystals grown under these conditions.

The scales grown in a water/hydrogen atmosphere show oxide ridges (see fig. 4). Similar oxide ridges were also observed by Hsu and Yurek[5] in cobalt oxide scales formed on cobalt in pure oxygen.

These oxide ridges are assumed to be due to preferred transport along oxide grain boundaries during oxidation. Similar to cobalt oxide, the holes between the oxide ridges are gradually filled with oxide. Figure 5 shows a side view on a stripped oxide scale, indicating that only the oxide adjacent to the oxide-gas interface shows a porous structure.

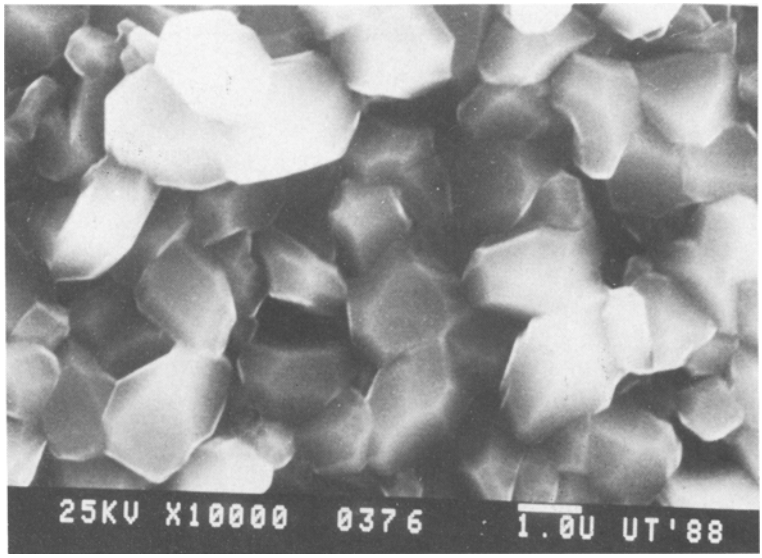

Fig. 2. Chromium oxide after oxidation at 900°C in O_2 for 15 hr.

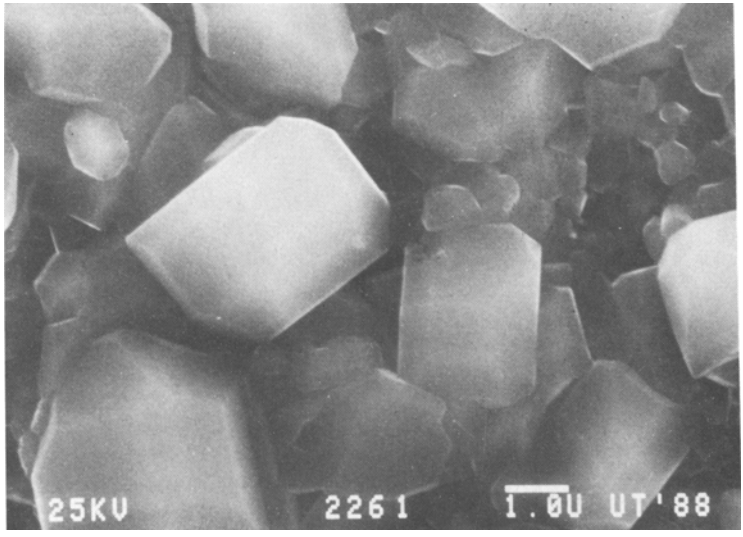

Fig. 3. Chromium oxide after oxidation at 900°C in O_2 for 15 hr.

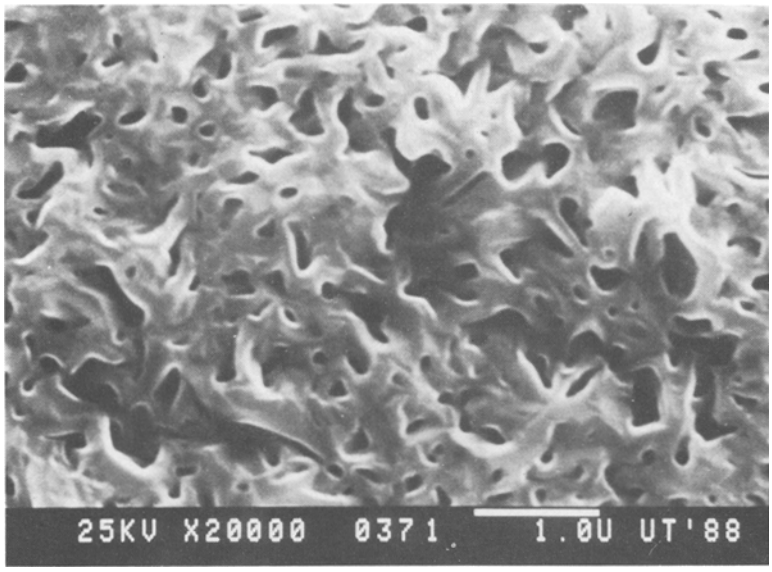

Fig. 4. Oxide ridges on chromium oxide after oxidation in H_2O/H_2 at 900°C for 15 hr.

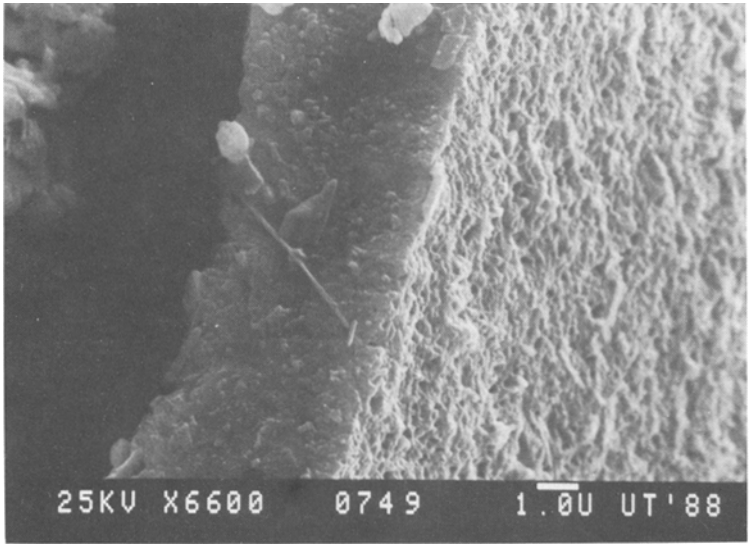

Fig. 5. Side view of chromium oxide after oxidation in H_2O/H_2 at 900°C for 15 hr.

Another feature appearing on oxide scales grown in H_2/H_2O is the presence of whiskers (see Fig. 6). This whisker formation was not observed on chromia scales grown in pure oxygen. Yurek[6] has observed whisker formation for oxidation of chromium in H_2/H_2O at 1025°C and noticed that this only takes place if the surface is mechanically polished but not if the chromium is electropolished or lightly etched before oxidation. Raynaud and Rapp[7] proposed that whisker growth occurs from screw dislocations emerging from the surface. They also found that the addition of water to pure oxygen at 1110°C leads to whisker formation on top of grains of nickel oxide grown on pure nickel.

The formation of oxide ridges and whiskers is also observed during the oxidation of chromium in a mixture of 1% CO in CO_2. The oxide ridge formation is less pronounced than in a 1.5% H_2O/H_2 mixture. The whiskers formed in CO/CO_2 are shorter and thicker. The oxide ridges and whiskers formed after oxidation in CO/CO_2 are shown in Fig. 7.

Chromia scales fail readily. Scale wrinkling is a common feature of chrmoia scales and is assumed to be due to lateral oxide growth caused by oxide growth within the scale. The appearance of scale wrinkling of a chromia scale formed after oxidation in pure oxygen is illustrated in Fig. 8. These oxide scales have an enormous ability to deform. For all oxidation experiments, no scale cracking during oxidation was observed. The ability

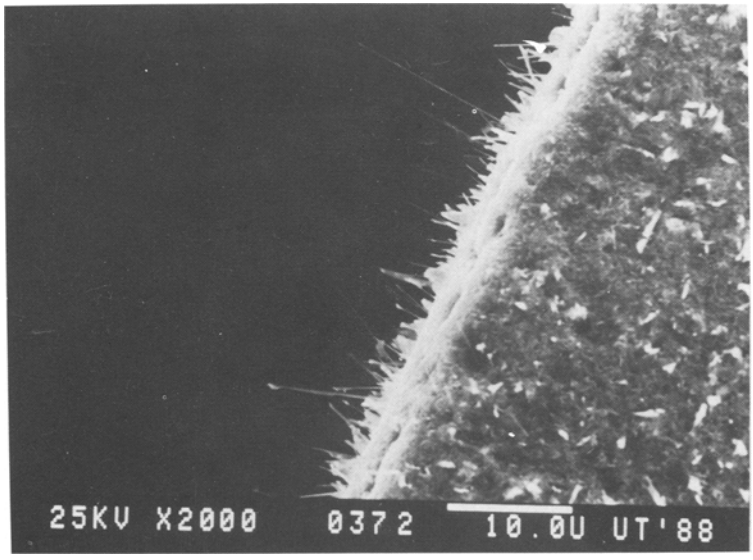

Fig. 6. Oxide-whisker formation after oxidation in H_2O/H_2 at 900°C.

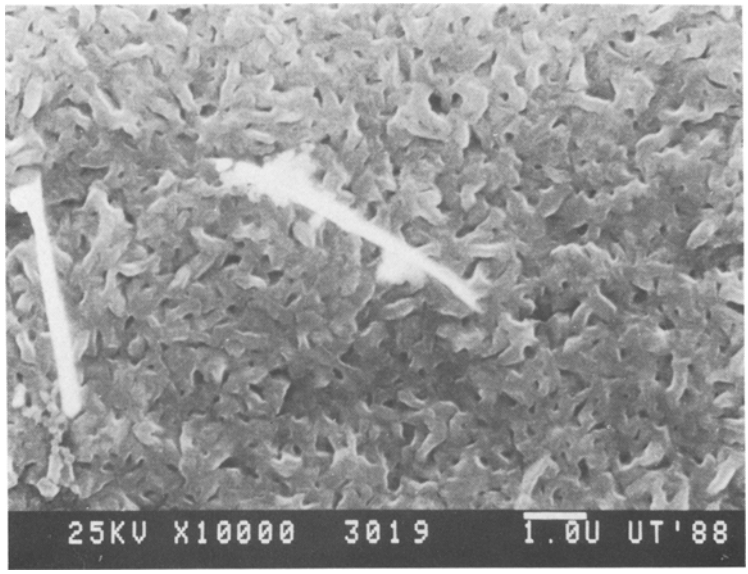

Fig. 7. Oxide-ridge and whisker formation after oxidation in CO/CO_2 at 900°C.

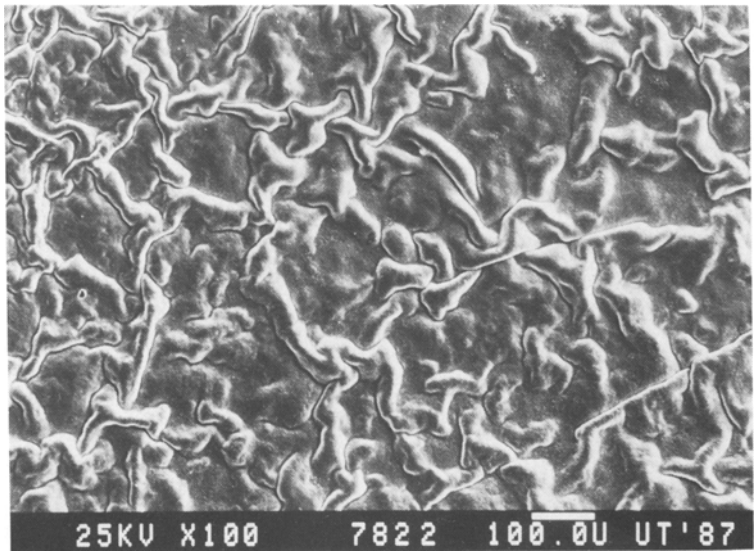

Fig. 8. Scale wrinkling after oxidation in O_2.

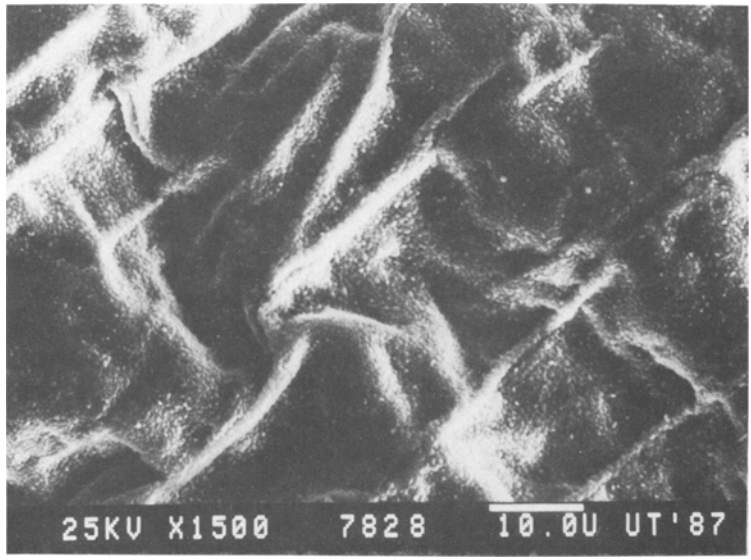

Fig. 9. Underside of a heavily buckled oxide scale.

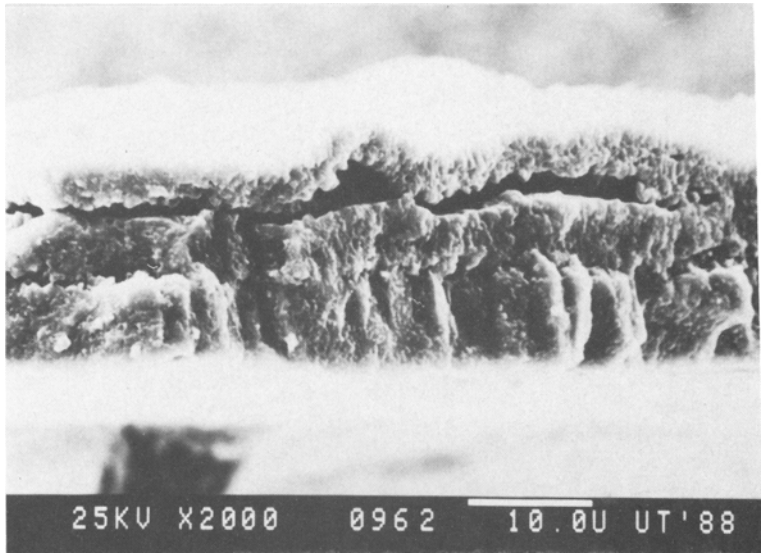

Fig. 10. Side view of an oxide scale that underwent scale breakdown.

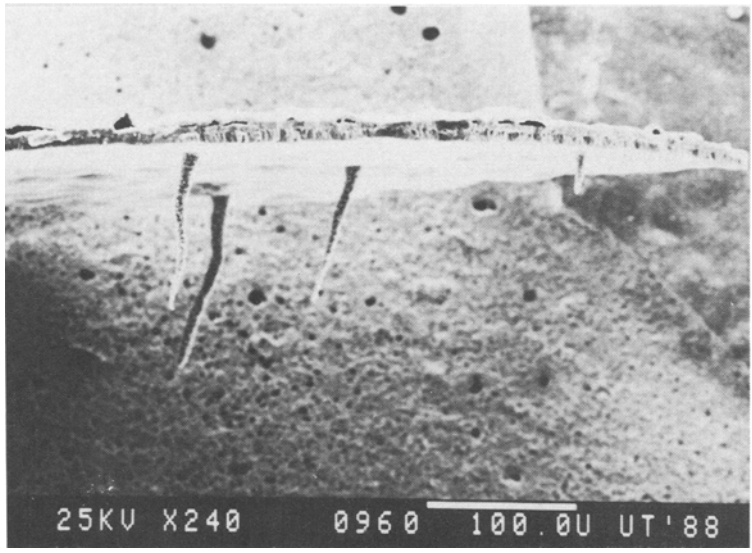

Fig. 11. Oxide pegs formed after scale breakdown.

to deform plastically was previously observed by Kofstad and Lillerud[1,2] and is further illustrated by Fig. 9, showing the heavily buckled chromia scale at the metal/oxide side.

Although no scale cracking was observed during the limited time of the oxidation experiments, the chromia scales may spall upon cooling at a rate of 30°C/hr.

Scale-cracking was created by oxidizing a sample in O_2 at 900°C, cooling it to room temperature at a rate of 30°C/hr, heating to 900°C at a rate of 30°C/hr, and oxidizing again. Figure 10 shows a side view of a stripped oxide scale formed on chromium that underwent this oxidation treatment. Several oxide layers are visible, probably formed after each scale breakdown. Another feature of cracked oxide scales is shown in Fig. 11. Oxide pegs form at the alloy grain boundaries after scale cracking. Oxide pegs were also noticed for noncracked scales, but then the length of these pegs is not more than a micrometer.

DISCUSSION

The oxidation mechanism of chromium is not fully clear, although it has been the subject of several experiments and discussions. However, there is a general support for the idea that grain-boundary diffusion of chromium defects is the main transport mechanism for the oxidation of chromium.[8-11]

As shown by the oxidation curves at 900°C, the oxidation kinetics at various oxygen partial pressures, may be described by Wagner's parabolic rate law. According to Wagner's theory, the rate of a transport of a component in the oxide scale is proportional to the electrochemical potential gradient of that component. If it is assumed that the possible defect mechanisms at the grain boundaries are the same as for the bulk, the predominant chromium transport can be explained either by chromium interstitials or chromium vacancies. Only the chromium-interstitial mechanism is able to explain that the parabolic rate constant is independent of the oxygen partial pressure if oxygen defects may be ruled out.

The suggestion for predominant chromium-interstitial migration in the oxide scale was made by Kofstad and Lillerud,[1] who observed only a slight dependence of the oxidation rate of chromium on the oxygen partial pressure at 1000°C, where the oxidation at low P_{O_2} was even faster than at 1 atm O_2.

The densification of chromia scales during a high-vacuum treatment was also explained by a chromium-interstitial mechanism.[2]

Hindham and Whittle[3] found chromium oxidation to be completely independent of P_{O_2} at 1000°C in CO/CO_2 mixtures at $2\times10^{-14} < P_{O_2} < 8\times10^{-9}$ bar, and supported the chromium-interstitial model proposed by Kofstad and Lillerud. The oxidation experiments at 900°C presented in this paper also show that the oxidation kinetics are practically independent of P_{O_2} for a wide range of partial pressures.

The oxidation phenomena may be explained by the defect model proposed by Kofstad and Lillerud[1] who assumed that chromium interstitials predominate in the oxide scale near the alloy/oxide interface and that the outer region shows intrinsic electronic conduction. In this model, chromium vacancies may be the majority of defects very near the oxide/gas interface, but the total amount of vacancies is too low to influence the oxidation rate. The model of Kofstad and Lillerud allows the determination of the parabolic rate constant from the concentration gradient of the chromium interstitials. The parabolic rate constant is then related to the amount of interstitials in the oxide near the metal and, according to Wagner's parabolic rate equation, can be formulated to be

$$k_p = (\alpha+1) D_{Cr^0} \{ (P^i_{O_2})^{-3/4(\alpha+1)} - (P^g_{O_2})^{-3/4(\alpha+1)} \} \qquad (1)$$

where D_{Cr^0} is the self-diffusion coefficient of chromium in chromia in equilibrium with oxygen at unit activity, $P^i_{O_2}$ and $P^g_{O_2}$ are the effective oxygen partial pressures at the inner-(metal side) and outer- (gas side) scale interfaces, and α is the charge of the chromium-interstitial defect.

Since $P^i_{O_2}$ is the dissociation pressure of chromia in contact with chromium, and $P^g_{O_2}$ is practically always a few orders greater than $P^i_{O_2}$, Eq.

1 can be rewritten as

$$k_p \approx (\alpha+1) D_{Cr^0} (P^i_{O_2})^{-3/4(\alpha+1)} = (\alpha+1) D^i_{Cr} \tag{2}$$

This means that a chromium-interstitial mechanism leads to an oxidation behavior independent of the oxygen partial pressure.

A predominant chromium-vacancy-defect mechanism results in a parabolic rate constant that can be formulated to be

$$k_p = (\alpha+1) D_{Cr^0} \{(P^g_{O_2})^{3/4(\alpha+1)} - (P^i_{O_2})^{3/4(\alpha+1)}\} \tag{3}$$

and gives rise to an easily measurable dependence of k_p on the oxygen partial pressure, because $P^i_{O_2} \ll P^g_{O_2}$.

The validity of the proposed chromium-interstitial mechanism is doubtful following the Seebeck measurements of Young *et al.*[4] They observed for sintered chromia that equilibration with the ambient oxygen partial pressure, especially the transition from *p*-type material to *n*-type material, only takes place at very high temperatures (1500°C and higher). Hence equilibration will not take place within the oxide scale at 900–1000°C. Especially after scale breakdown or scale cracking, it is unlikely that the new oxide formed within the scale will transform to *n*-type and that chromium interstitials will still be the predominant defects. The Seebeck experiments of Young *et al.*[4] may represent the behavior of the bulk of the oxide; therefore, it is possible that equilibration does take place at the grain boundaries of the oxide.

The SEM pictures show the tendency for chromia crystals to form clusters of smaller crystals in pure oxygen. This is in agreement with grain-boundary simulations and calculations.[12] The calculations revealed a decrease in surface energy if a tilt- or twin-grain boundary was formed.

The oxygen for the oxidation of chromium at 900°C in 1% CO/CO_2 and in 1% H_2O/H_2 must be supplied by CO_2 and H_2O, respectively, and not by O_2. A rough estimate of the surface coverage of O_2 in a H_2/H_2O mixture, with a P_{O_2} of 1×10^{-20} bar can be made using the chemisorption enthalpies of O_2 on chromia of Joly *et al.*[13] determined at 500°C. If this adsorption enthalpy of 150 kJ/mol is also valid at 900°C, and if the adsorbed O_2 is considered as a two-dimensional gas, then the surface coverage Θ calculated by the Langmuir adsorption isotherm

$$\Theta = (b_a\, e^{-\Delta Hads/RT}) \times P/(1 + b_a\, e^{-\Delta Hads/RT} \times P) \tag{4}$$

would be approximately 7×10^{-19}. In Eq. 4, P and b_a are the oxygen partial pressure and the equilibrium constant for adsorption, respectively. This low surface coverage can never account for the observed oxidation rates. If the adsorption of O_2 would be rate determining, no parabolic kinetics are

expected. The diffusion of some defect species has to be rate-determining in view of the observed parabolic kinetics and not the adsorption of an oxygen-containing species from the gas phase. Therefore, the oxidation in CO/CO_2 and H_2/H_2O can take place only by chemisorption of CO_2 and H_2O on the chromia surface. The species predominantly chemisorbed might lead to different scale morphologies as demonstrated in the next section.

Raynaud and Rapp[7] developed a theory for the whisker formation of NiO in moist oxygen. According to this theory, whiskers grow by surface diffusion of cations along a tunnel centered around the core of a screw dislocation or a bundle of dislocations (see Fig. 12), and our observations are in agreement with this theory.

TEM studies by Voss *et al.*[14] confirmed the existence of a central hollow tunnel within α-Fe_2O_3 whiskers grown on iron from 600–800°C. Rapp and Raynaud suppose that the surface diffusion D_s is very fast, and that the dissociation of the molecular oxidant is the rate-limiting step for whisker growth. Evidence for this theory was supplied by the determination of the activation energy for the initial oxidation of iron to wustite by Turkdogan *et al.*[15] who calculated the energy of activation for the initial stage of oxidation where the chemisorption or dissociation of oxidant molecules is assumed to determine the oxidation process of iron. They found that the activation energy at 850–1150°C was 80.3 kJ/mol in H_2/H_2O, much lower than the value determined for oxidation in CO/CO_2 mixtures (217.4 kJ/mol). Experimental data for the activation energy of the chemisorption or dissociation of O_2, H_2O, and CO_2, respectively, on

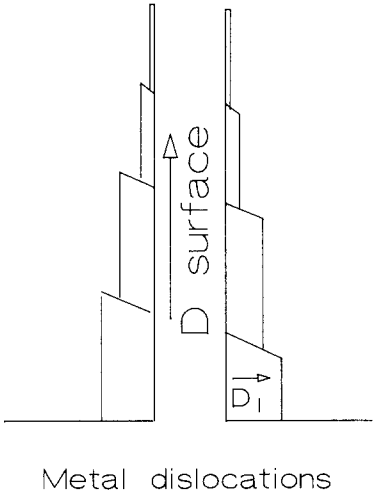

Fig. 12. Proposed model for whisker formation (Ref. 7); D_s is the surface diffusion in the tunnel, and D_l the lattice diffusion.

chromia are not available. A similar theory might be applicable to explain the whisker formation on chromia surfaces. The activation energy of chemisorption or breakup at 900°C for chromium oxidation should then be according to the order: $E_{act}(H_2O) < E_{act}(CO_2) < E_{act}(O_2)$.

For the formation of oxide ridges at the grain boundaries of oxide grains in H_2/H_2O and CO/CO_2 mixtures as shown in Fig. 6, this mechanism may also be applicable. The cation diffusion at the oxide grain boundaries is fast compared to lattice diffusion. For grain-boundary diffusion, the dissociation of the oxidant molecule may be also rate-limiting. Hsu and Yurek[5] observed oxide ridges for the oxidation of Co in O_2 at 600–800°C. According to Hsu and Yurek, the preferential growth over grain boundaries cannot occur indefinitely, because the diffusion distance in the protrusions of Cr_2O_3 becomes finally large enough to favor growth at the base of the ridges. Consequently, these ridges are of limited height, and hence this might be the reason for the absence of pores in the bulk of the oxide. A schematic drawing of the model proposed by Hsu and Yurek is given in Fig. 13.

The formation of oxide pegs after scale breakdown takes place at the metal, multiple-grain junctions, where the supply of metal defects is very fast. After scale breakdown these voids at the metal, multiple-grain junctions are preferentially oxidized, leading to the formation of large oxide pegs (see Fig. 14).

The formation of wrinkled oxide scales is assumed to take place by lateral oxide growth, caused by oxide formation within the oxide scale.[16] It is not likely that this internal oxidation is taking place by inward diffusion of oxygen defects through the oxide scale. The ^{18}O tracer diffusion experiments of Skeldon *et al.*[17] at 950°C, and of Cotell *et al.*[18] at 900°C, show that, up to an oxide scale thickness of about 1 μm, 99% of the mass transport in the oxide scale may be attributed to outward growth caused by transport of chromium defects. The inward growth for thicker scales, observed by

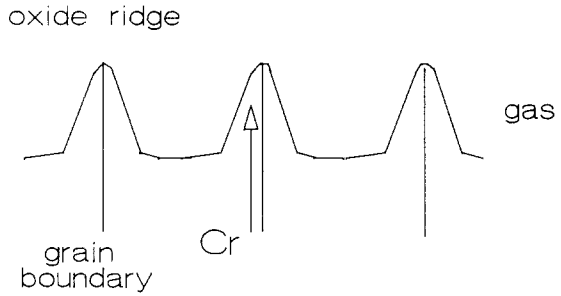

Fig. 13. Proposed model for oxide-ridge formation (Ref. 5).

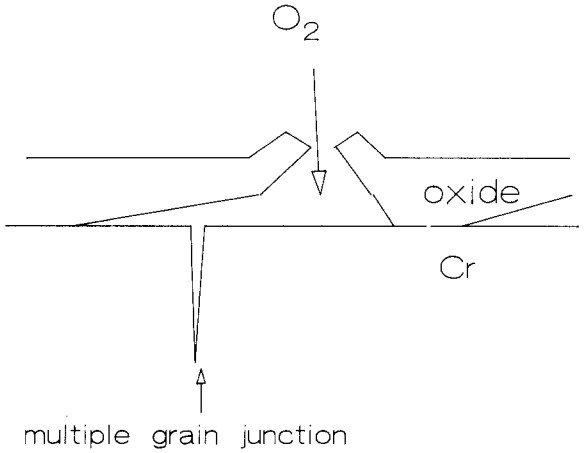

Fig. 14. Oxide-peg formation after scale breakdown.

Skeldon *et al.*,[17] is probably not caused by a change over in the solid-state-diffusional mechanism, but by oxygen transport through pores and micro channels, in accordance with the mechanisms described by Kofstad.[19]

A summary of the oxidation of chromium shows the following characteristics:

1. Chromium oxidation takes place predominantly by outward growth, and the scale-growth kinetics are parabolic at least for limited scale thicknesses. The exact defect mechanism is not clear, but is independent of the external oxygen partial pressure.
2. After reaching a certain scale thickness, some inward oxide growth takes place by pores and micro channels. Thermal shocks applied to oxide scales or the formation of very thick oxide scales give rise to scale breakdown and the formation of oxide pegs.
3. Oxidation of chromium in CO/CO_2 or H_2/H_2O mixtures causes oxide-whisker formation and oxide-ridge formation at the oxide grain boundaries. Oxide ridge and whisker formation do not result in a significant change of the oxidation kinetics.

ACKNOWLEDGMENTS

Most of the pictures presented in this paper were obtained by the skilful handling of Dr. B. A. Boukamp and Ing. B. Geerdink.

REFERENCES

1. P. Kofstad and K. P. Lillerud, *J. Electrochem. Soc.* **127**, 2410 (1980).
2. P. Kofstad and K. P. Lillerud, *Oxid. Met.* **17**, 177 (1982).
3. H. Hindham and D. P. Whittle, *J. Electrochem. Soc.* **130**, 1519 (1983).
4. E. W. A. Young, J. H. Gerretsen, and J. H. W. De Wit, *J. Electrochem. Soc.* **134**, 2257 (1987).
5. H. S. Hsu and G. J. Yurek, *Oxid. Met.* **17**, 55 (1982).
6. G. J. Yurek, in *Corrosion Mechanisms*, F. Mansfeld, ed. (Marcel Dekker, New York, 1987), p. 397.
7. G. M. Raynaud and R. A. Rapp, *Microstruct. Sci.* **12**, 197 (1985).
8. E. A. Polman, T. Fransen, and P. J. Gellings, *J. Phys. C*, in press (1989).
9. A. Atkinson and R. I. Taylor, *NATO ASI Series* **B129**, 285 (1984).
10. K. Hoshino and N. L. Peterson, *J. Am. Ceramic Soc.* **66**, C202 (1983).
11. P. Kofstad and K. P. Lillerud, *Oxid. Met.* **17**, 177 (1982).
12. E. A. Polman, thesis, University of Twente (1989).
13. J. P. Joly, *J. Chimie Phys.* **72**, 1019 (1975).
14. D. A. Voss, E. P. Butler, and T. E. Mitchell, *Metallurg. Trans.* **13**, 929 (1982).
15. E. T. Turkdogan, W. M. McKewan, and L. Zwell, *J. Phys. Chem.* **69**, 327 (1965).
16. P. Kofstad, in *High Temperature Corrosion* (Elsevier Applied Science Publishers, Essex, 1988), Ch. 12.
17. M. Skeldon, J. M. Calvert, and D. G. Lees, *Oxid. Met.* **28**, 109 (1987).
18. C. M. Cotell, G. J. Yurek, R. J. Hussey, D. F. Mitchell, and M. J. Graham, *J. Electrochem. Soc.* **134**, 1871 (1987).
19. P. Kofstad, *Oxid. Met.* **24**, 265 (1985).